Engineering Coking-Resistant Catalysts in the Dry Reforming of Methane: Effect of Catalyst Structure

Titus Lim Jing En
School of Chemical and Biomolecular Engineering

Asst. Prof Tej Salil Choksi
School of Chemical and Biomolecular Engineering
Lavie Rekhi (PhD)
School of Chemical and Biomolecular Engineering

Abstract - In recent years, the harmful effects of greenhouse gas emissions (global warming, overall environmental destruction) have attracted the attention of organisations and the public. Thus, greenhouse gas conversion into useful by-products for manufacturing purposes has been gaining the interest of researchers. One of the many reactions is the Dry Reforming of Methane (DRM), which converts CO_2 and CH_4 into syngas: An important precursor in producing liquid fuels like diesel [3]. This reaction is catalysed by Earth-abundant metal catalysts like nickel which have been extensively studied to date. Despite that, they are susceptible to coking and sintering at the high temperature and pressure conditions of DRM [6]. Current advancements in catalysis technology are also limiting the possibility of significant breakthroughs in understanding catalytic behaviour in DRM. This study focuses on the vanadium carbide catalyst (particularly the Miller plane surface VC (110)), reducing coking on it by adsorbing oxygen atoms (ranging from 1 to 12) on different adsorption sites on the catalyst surface. Computational modelling is used to create simulations of the altered chemical structure of the catalyst (and obtain the experimental results for said simulations). From preliminary findings, adsorbing 12 oxygen atoms on the vanadium-carbon bridge site gives the most stable catalyst structure amongst other sites. Generally, increased oxygen surface coverage is positively correlated with vanadium carbide catalyst stability from the Ab-initio phase diagrams constructed (A phase diagram is a graphical illustration of a substance's property at a certain temperature and pressure).

1 INTRODUCTION

1.1 BACKGROUND

Climate change is evolving to be a major problem of this century. The gradual warming of the Earth has led to a rise in sea levels over the past decade, which directly threatens Singapore's low-lying lands [4]. In addition, excessive global warming affects the ecosystem as well as the livelihood of Singaporeans due to variability of the weather. Erratic weather patterns can also cause flash floods occurrences and drastic weather patterns, which can overwhelm the nation's water drainage system [4].

One of the reasons cited for global warming is carbon emissions, which traps heat from radiating outside of the Earth's atmosphere due to the greenhouse effect [4]. This implies that achieving net-zero emissions could significantly negate the negative consequences of global warming, which is in line with Singapore's decarbonization roadmap [4]. Out of the 4 major components outlined in the roadmap, the Dry Reforming of Methane (DRM) is related to the area of hydrogen production.

Hence, this paper focuses on DRM, one of the key industrial reactions to produce valuable syngas (a mixture of carbon monoxide and hydrogen gases) - a precursor of liquid fuels and chemicals production. As DRM is a heterogenous catalytic reaction (since reactants and products are gases), the catalyst studied will be the vanadium carbide (VC) catalyst. In detail, the 110 Miller plane surface of the catalyst will be the central focus. In addition, one of the ways to reduce coking: increasing oxygen concentration, will be explored later in this report.

1.2 DRM DETAILS

DRM is no stranger to heterogenous catalysis: studies have been conducted using various catalysts, such as MXene-based catalysts (2D transition metal carbides and nitrides) and transition metal oxy – carbide catalysts to increase catalytic efficiency of DRM [5]. Recently, DRM is also seen to be a straightforward approach to effective CO2 conversion, on top of producing added value syngas [3]. The reaction equation is shown below:

$$CH_4 + CO_2 \leftrightarrow 2CO + 2H_2 \quad (1)$$

Thermodynamically, high syngas conversion is theoretically feasible at harsh conditions of temperatures above 800^{o}C as DRM is an endothermic reaction [3]. Kinetically, the reaction mechanism depends on the rate-determining (the slowest) step, which is usually methane adsorption

on the catalyst surface [3]. The entire reaction mechanism can be briefly summarized in order as: methane adsorption, reaction between methane and atmospheric carbon dioxide, and syngas desorption. This is the first problem of coking: harsh DRM conditions also encourages methane decomposition, driving carbon residue formation on the catalyst surface [6]. In addition, the catalysts may not be thermally stable enough to withstand degradation at high temperatures, leading to defects formed at the catalyst surface. This hinders product formation on the surface at the reaction phase of the mechanism, which means the catalyst active sites are not efficiently utilized [4]. This is the second problem of sintering.

This paper starts by focusing specifically on vanadium carbide catalysts. This study aims to address the first problem of coking, by adsorbing oxygen atoms on the catalyst surface. A few implicit assumptions are made to narrow down the possibilities: Only the Miller plane surface VC (110) will be used in the computations; only oxygen atoms will be adsorbed on the catalyst surface; only simple geometries of catalyst adsorption sites are considered, like the VC-bridge site and the V-top or C-top sites; a reaction temperature of 548K will be used to determine the most stable oxygen surface coverage from the ab-initio phase diagrams.

1.3 APPROACH

This study is entirely based on computational simulations. The approach is as follows: computational modelling followed by catalyst stability comparisons using multiple phase diagrams, constructed at a temperature of 548K. Density functional Theory (DFT), a quantum mechanical modelling method, is used alongside thermodynamic calculations to aid in catalyst stability checks.

Firstly, DFT is used to determine the most stable VC catalyst adsorption site, out of a few conventional ones (VC – bridge, C – top, V – top, VV – bridge etc.). These examples are illustrated in the below figures:

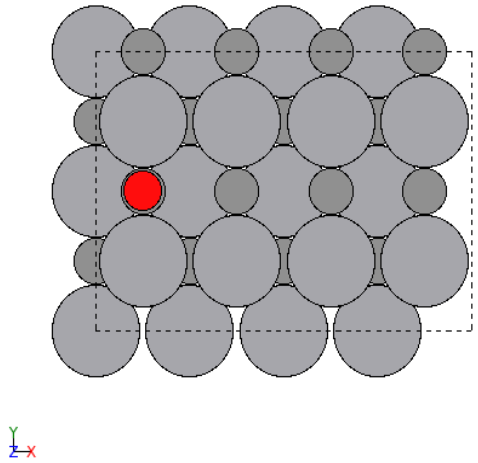

Figure 1 C – top adsorption site

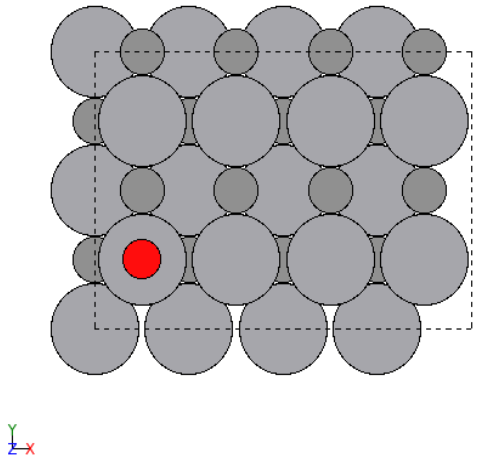

Figure 2 V – top adsorption site

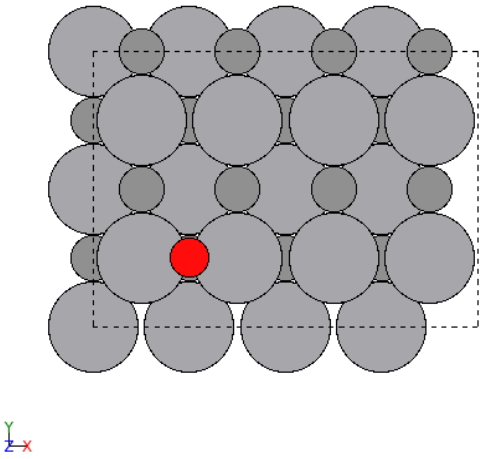

Figure 3 VV – bridge adsorption site

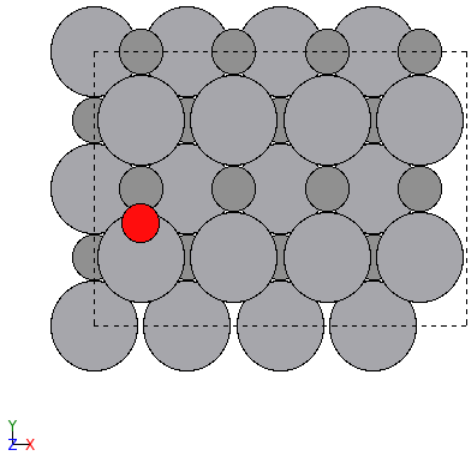

Figure 4 VC – bridge adsorption site

To interpret the above 4 figures, the larger grey circle is the vanadium (V) atom; the smaller dark grey circle is the carbon (C) atom, and the red circle is the oxygen (O) atom. Table 5 below shows the ground – state energy values obtained from the DFT calculations with 1 oxygen atom as the adsorbate. The oxygen atom is positioned at a height of 2 Å (angstroms) above the VC (110) surface for the DFT calculations.

Config	Energy (eV)
C-top	-85657.514822
V-top	-85657.126934
V-C-bridge	-85658.383587
V-V-bridge	-85657.775384

Table 5 Selected DFT Energy Values

From Table 5, it is apparent that the ground – state energy of the VC (110) bridge adsorption site is the lowest. Thus, the VC (110) bridge site stabilizes the VC (110) structure to the greatest extent compared to the rest of the adsorption sites listed.

Secondly, at the most stable VC site determined, up to 12 oxygen atoms will be adsorbed onto the VC surface. DFT is then used again to determine the most stable number of adsorbed oxygen atoms on the VC catalyst. Lastly, thermodynamic calculations will be carried out to construct multiple phase diagrams from the energy data collated from DFT. The most stable VC catalyst structure will be determined at a desired pressure and temperature.

In detail, the thermodynamic calculations involve the calculation of the grand potential of a particular VC (110) – nO surface. The formula for the grand potential is as follows:

$$\Delta\Omega = E_{VC-nO*} + n_O ZPE_{O*} - n_O TS_{O*} - \mu_{VC} - n_O\mu_O \quad (2)$$

$$\mu_{VC} = E_{VC\,(100)} \quad (3)$$

$$\mu_O\,(T,P) = E_{O2}^{Gas} + ZPE_O - TS_{O2}^{o}(T,P_{O2}) + RT\ln\left(\frac{P_{CO2}}{P_{CO}}\right) \quad (5)$$

2 MAIN CONTENT

2.1 THE DENSITY FUNCTIONAL THEORY (DFT) METHOD

DFT is the main computational modelling method used in this report. Specifically, DFT aids in producing atomistic simulations of the electronic structure of a given system, by performing ab-initio (by first principles) thermodynamic calculations without the need for experimental input. The completion of the calculations allows for the prediction of certain chemical properties of the system (stability, reaction rates) with sufficiently high accuracy. In addition, DFT can also predict the chemical properties of a previously unknown chemical system.

The foundation of DFT is built on solving the time-independent Schrodinger equation: a complex equation involving the wave functions of all N electrons in the system [2]. The equation is shown below:

$$\hat{H}\Psi = E\Psi \quad (4)$$

The Schrodinger equation consists of 3 parts: the Hamiltonian operator $\hat{H}$, the ground-state energy of all N electrons E, and the energy eigenstates of the Hamiltonian Ψ [2]. Ψ is also known as the electronic wave function, which is a function of each of the N electrons' spatial coordinates (x, y and z) in a 3D space. The Hamiltonian is derived from the principle of conservation of energy in quantum physics rather than classical physics (classical kinetic energy considers mass and velocity, while quantum kinetic energy considers mass and momentum). The direct solution is obtained by solving for all unknown coordinates of N electrons, given the fixed position of each atom. For a set of N electrons moving within the atomic system, the minimum energy state (or ground state) of the electrons can be found [2].

The complexity of Schrodinger's equation means that direct solutions are impractical to achieve. Each electron exists in the 3D space (x, y and z coordinates), and since there are N electrons in an arbitrary chemical system, 3N dimensional wave functions in the equation will have to be solved (this means that, for an atomic system of N electrons, 3N coordinates of all electrons will have to be computationally determined). The computational expense of a direct solution is hence highly impractical.

Currently, DFT has been refined such that calculations using computers are feasible. The Hohenberg-Kohn theorems and the Kohn-Sham equations relaxed the requirement to solve for all

3N coordinates of electrons directly [2]. The Kohn-Sham equations outline an iterative method in finding an approximate solution to the Schrodinger equation, rather than a direct solution. The first Hohenberg-Kohn theorem proved that: *The ground-state energy from Schrodinger's equation is a unique functional* (mathematically, a functional is the definite integral of a function f(x) [2]. Thus, a functional produces a single number that is unique to every value input in f(x)) *of the electron density* (electron density is a measure of the probability of finding an electron in a region of space, in an atom or molecule. The higher it is, the more likely an electron is there). Essentially, the theorem implies that the ground-state electron density is uniquely related to all ground-state properties, like the wave function Ψ and the ground-state energy E. This reduces the problem of solving for 3N coordinates in the Schrodinger's equation, to just solving for the ground-state electron density of a given system, and hence the ground-state energy E of said system. The number of unknowns changes from 3N coordinates, to just 3 coordinates x, y, and z (since the electron density is a function of the position vector $r(x, y, z)$). The second theorem proves that the full solution of Schrodinger's equation is the electron density that minimizes the energy of the overall functional [2].

Theoretically, the calculations work in this manner: An initial guess of the electron density is defined to solve the Kohn-Sham equations. The electron density is also calculated from the wave functions of the Kohn-Sham equations, which is compared to the initial guess. An approximate solution is reached when both electron densities converge close to each other, which is determined by the researcher at task. This is the underlying method by which DFT handles its calculations and arrive at the converged solution. From the second Hohenberg-Kohn theorem, the converged solution finds the minimum energy (ground-state energy) of the system which is the point of interest in this report [2]. The most stable chemical and physical properties of an atomic system can be predicted from the structure at its ground-state energy, which is provided with the aid of simulations from the DFT computations.

With respect to this report, the atomic system of interest is the vanadium carbide catalyst consisting of vanadium and carbon atoms arranged alternately as shown below:

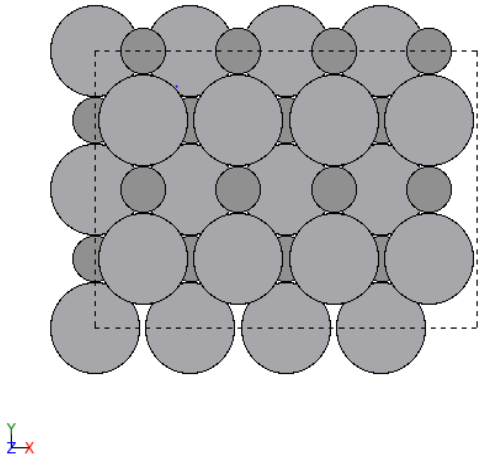

Figure 6 VC (110) – clean surface

The surface of focus is the (110) surface of the VC catalyst structure.

To increase the ease of computation, only 5 layers of vanadium and carbon atoms (constituting 1 slab model of the VC catalyst) is used as the given system for DFT calculations. In addition, only 1 unique surface of the VC catalyst, corresponding to the Miller Plane (110), will be analyzed. Up to 12 oxygen atoms will be adsorbed onto the VC (110) surface, simulated by manually adding oxygen atoms onto the surface.

2.2 RESULTS & DISCUSSION

The following table (Table 1) shows the converged energy values of each VC (110) catalyst slab with the adsorbed oxygen atoms (ranging from 1 to 12 adsorbed oxygen):

# of Oxygen	Oxygen Surface Coverage	Energy/eV	Avg. BE/eV	Diff. BE/eV
1	0.06	-85658	-3.92	NA
2	0.13	-86098	-3.09	-2.25
3	0.19	-86539	-3.13	-3.21
4	0.25	-86980	-3.26	-3.66
5	0.31	-87421	-3.37	-3.80
6	0.38	-87862	-3.38	-3.42
7	0.44	-88303	-3.42	-3.66
8	0.50	-88745	-3.51	-4.12
9	0.56	-89184	-3.27	-1.36
10	0.63	-89625	-3.31	-3.72
11	0.69	-90063	-3.07	-0.63
12	0.75	-90503	-3.03	-2.58

Table 7 DFT Energy Values (eV) against number of adsorbed oxygen atoms

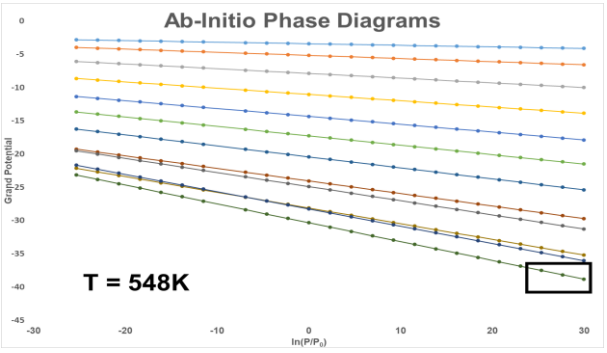

Figure 8 Ab – Initio Phase diagrams at a temperature of 548 K

From the phase diagrams, it is observed that the grand potential of the VC (110) – 12O surface (corresponding to the black box region) is the lowest among all the VC (110) – nO surfaces. Thus, at a temperature of 548 K, it is concluded that the most stable oxygen surface coverage is the surface that has 12 oxygen atoms adsorbed on it.

From Table 7, there is a clear downward trend in the internal energies of the catalyst slab: As the number of surface oxygen atoms increases, the internal energy of the structure decreases. Thermodynamically, this means an increase in stability of the catalyst structure. Thus, it is concluded that the most stable number of adsorbed oxygen atoms on the VC (110) surface is 12 (within the assumptions of this report).

From the internal energy values, the average and differential binding energies (BE) of each surface are also calculated. Mathematically, both binding energies are calculated as shown below:

$$Avg.BE = E_{VC\ (110)-nO} - E_{VC\ (110)} - (nO)/2 * E_{O2\ (g)} \quad (5)$$

$$Diff.BE = E_{VC\ (110)-(n+1)O} - E_{VC\ (110)-nO} - (nO)/2 * E_{O2\ (g)} \quad (6)$$

E_{VC-nO} represents the internal energy of the VC slab with n surface oxygens; $E_{VC-(n+1)O}$ represents the internal energy of the VC slab with (n+1) surface oxygens; E_{VC} represents the internal energy of the VC slab with a clean (110) surface; (nO) represents the number of surface oxygens adsorbed on any VC (110) surface, and $E_{O2\ (g)}$ represents the internal energy of gaseous oxygen in its molecular state. Theoretically, average BE measures the averaged amount of energy required for the adsorption of 1 oxygen atom on the catalyst surface, while differential BE calculates the additional energy required to adsorb 1 more oxygen atom on a catalyst surface. For differential BE, the oxygen can be adsorbed on either a clean catalyst surface, or a surface with adsorbed oxygens.

From the 2 BE definitions above, one can make a few observations. Firstly, the average BE should be consistent across all VC (110) surfaces, regardless of the number of adsorbed oxygens. This is because the average energy required for the adsorption of a single oxygen atom should be within a certain confidence range (since the energy is experimentally determined, hence a range to account for random and systematic errors). Secondly, the differential BE should generally increase as the number of oxygen atoms adsorbed increases. On a clean VC catalyst surface, the oxygen atom only must overcome the electrostatic forces of repulsion between the valence electrons of surface vanadium and carbon atoms. In contrast, on a VC (110) – 3O surface, the incoming oxygen atom must overcome the repulsive forces between the electrons of the surface vanadium and carbon atoms, as well as that of the 3 surface oxygen atoms. Greater electrostatic forces of repulsion would imply a greater amount of energy required to bring the oxygen atom close enough to the catalyst surface for adsorption to occur, resulting in an increasing trend for differential BE.

As expected, the experimental results agree with the theoretical reasoning for average BE. The trends of the 2 binding energies are plotted against the number of adsorbed oxygen atoms below:

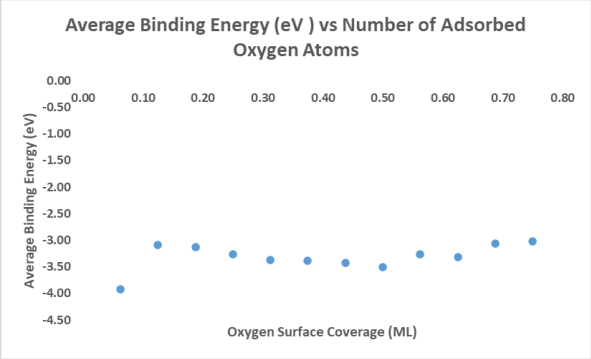

Figure 9 Average Binding Energy (eV) Trend

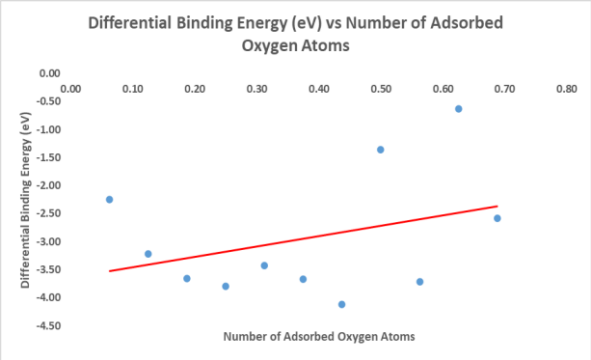

Figure 10 Differential Binding Energy (eV) Trend

From the plots (Figures 9 and 10), the x-axis is the oxygen surface coverage, measured in monolayers (ML). 1 ML constitutes to 16 oxygen atoms since the VC (110) surface has 16 VC – bridge adsorption sites; 0.5 ML constitutes to 8 oxygen atoms, and so on. The interpretation of the individual points in differential BE trend is as follows: For example, at 0.13 ML (2 oxygen atoms out of 16), the final number of adsorbed oxygen atoms is 2. From Table 1, the magnitude of differential BE (2.25 eV) is the amount of energy required to adsorb an additional oxygen atom on the VC (110) – 1O surface to create the final structure with the VC (110) – 2O surface.

From Figure 9, across all 12 VC (110) – nO surfaces, the average BE values consistently fall within a range of 3 – 4 eV. This is expected. From the Figure 10, the differential BE increases with

increasing number of adsorbed oxygen atoms, as expected from the theory. However, the individual points for differential BE highlight a counter – intuitive trend. The differential BE decreases steadily at 3 regions: 2O – 5O, 6O – 8O, 9O – 10O and 11O – 12O, even though differential BE is expected to increase. The following paragraphs focuse on the region of 2O – 5O, using the VC (110) – 2O surface as an example to explain the phenomenon observed.

The discrepancies between the theoretical and experimental observations could be explained by analyzing the simulation of each of the VC (110) – nO surfaces more closely. From formula (6), a decreasing trend in differential BE would mean that the rate of increase in ground-state energy of VC (110) – nO surfaces is decreasing as oxygen surface coverage increases. The trend also implies every additional oxygen adsorbed does not require a larger amount of energy to do so. Hence, this could mean that the electrostatic forces of repulsion between the oxygen atoms on the VC (110) surface and the incoming oxygen atom (to be adsorbed) is not as strong as intuitive reasoning suggests. For low surface coverages (2O – 5O), the smaller repulsive forces could be attributed to a low number of oxygen atoms present on the VC (110) surface. A smaller number of surface oxygen would allow newly adsorbed oxygen atoms to be slightly repelled horizontally across the surface, and not be strictly adsorbed to the VC – bridge site exactly. This is observed from the VC (110) – 2O surface after the DFT calculations converged:

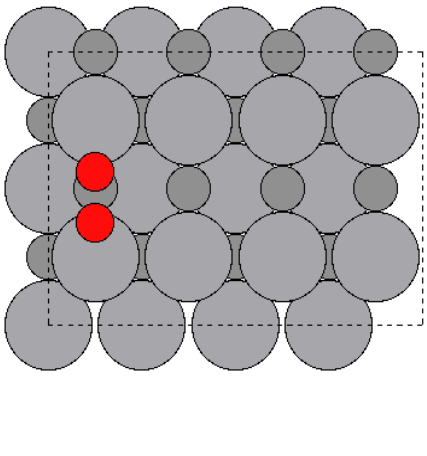

Figure 11 VC (110) – 2O surface, first DFT, before

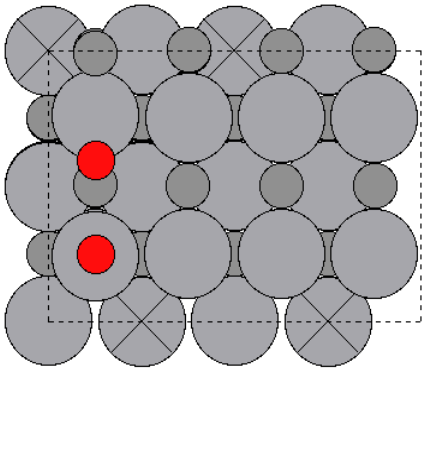

Figure 12 VC (110) – 2O surface, first DFT, after

From Figure 12, the most stable VC (110) – 2O structure has a surface with one of the oxygen atoms away from the VC – bridge site, and on the V – top site. This structure stabilizing behavior implies that adsorbed oxygen atoms do not adsorb very strongly onto the VC – bridge site (which as previously determined, is the most stable adsorption site). This alludes to the presence of more than one stable adsorption site other than the VC – bridge site, depending on the number of oxygen atoms as well as the configuration of oxygen atoms on the VC (110) surface. This hypothesis is tested by shifting the bottom-left oxygen atom to the boundary VC – bridge site and running another set of DFT calculations. As expected, the boundary VC – bridge site is a stable adsorption site for the bottom-left oxygen atom, as shown in Figures 13 and 14:

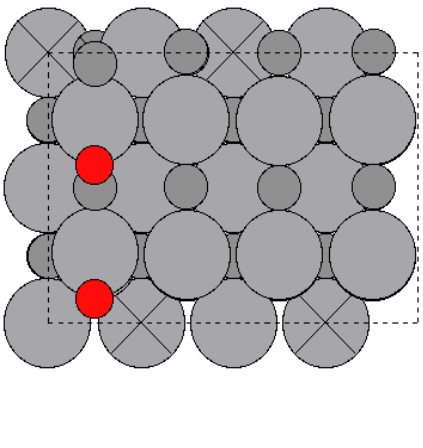

Figure 13 VC (110) – 2O surface, second DFT, before

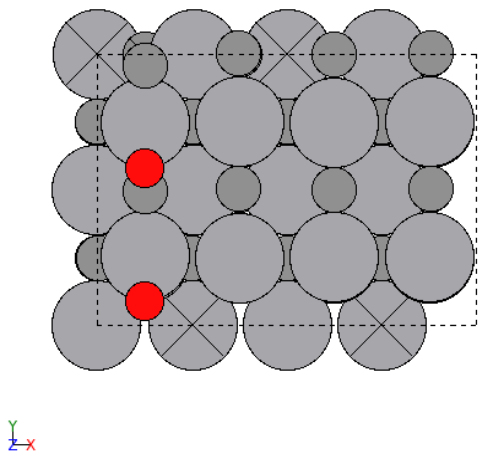

Figure 14 VC (110) – 2O surface, second DFT, after

To compare the relative stability of the structures from Figures 12 and 14, the converged ground – state energy values from the DFT calculations are compiled in Table 8:

Structure	Energy (eV)
Figure 12	-86098.099359
Figure 14	-86098.902520

As expected, the ground – state energy of the VC structure in Figure 14 is lower than that of Figure 12. This suggests that the VC – bridge adsorption site is more stable than the V – top site, which is an identical result found earlier.

3 CONCLUSION

In summary, the DFT method is used in this report to determine the most stable number of adsorbed oxygen atoms on the VC (110) surface. Additional thermodynamic calculations of the grand potential on the VC structure are conducted after the DFT computations, to determine the most stable VC (110) – nO structure, given a temperature of 548 K. For VC (110) surfaces with more than 6 surface oxygen atoms, additional DFT data is needed to explain the phenomenon observed from the simulations.

Moving forward, there are a few pointers that can help further the work discussed here and explain the DFT results better. Firstly, the Ab – initio phase diagrams' accuracy can be improved by adding more arrangements of surface oxygen atoms. This can be done by considering different oxygen atom configurations at each oxygen surface coverage. Improving the phase diagrams by supplying more results, contributes to an improved conclusion with respect to the most stable oxygen surface coverage for the VC (110) structure. Secondly, this report recorded the presence of more than one stable adsorption site at specific local sites on the VC (110) surface. In the example of 2 surface oxygen atoms in Figure 12, there is a locally stable V - top adsorption site in addition to the VC – bridge site. Exploring these locally stable adsorption sites can help explain or confirm the horizontally repelling behaviour which allows free movement of surface oxygen atoms, but at the expense of moving to a comparatively less stable adsorption site (considering the differences in ground – state energy in the example of Figures 12 and 14). Lastly, the current work of using oxygen as the adsorbate can be extended to include oxy – carbide structures, which are experimentally found to be coking – resistant based on current research [1].

ACKNOWLEDGMENT

I would like to acknowledge the funding support from Nanyang Technological University – URECA Undergraduate Research Programme for this research project.

REFERENCES

[1] A. Kurlov, E. B. Deeva, P. M. Abdala, D. Lebedev, A. Tsoukalou, A. C. Vives, A. Fedorov and C. R. Muller, "Exploiting two-dimensional morphology of molybdenum oxycarbide to enable efficient catalytic dry reforming of methane", Nature Communications, Vol. 11, No. 4920, pp. 1 – 11, 2nd October 2020. https://doi.org/10.1038/s41467-020-18721-0

[2] David S. Sholl and Janice A. Steckel, Density Functional Theory: A Practical Introduction, New Jersey: John Wiley & Sons, 2009.

[3] E. le Sache and T.R. Reina, "Analysis of Dry Reforming as direct route for gas phase CO2 conversion. The past, the present and future of catalytic DRM technologies", Vol. 89, 2021. *https://doi.org/10.1016/j.pecs.2021.100970*

[4] H.C. Lau, S. Ramakrishna, K. Zhang and Mohamed Z. S. Hameed, "A Decarbonization Roadmap for Singapore and Its Energy Policy Implications, 2021.

[5] R. Thakur, A. V. Mohammadi, J. Smith, M. Hoffman, J. Mancada, M. Beidaghi and Carlos A. Carrero, "Insights into the Genesis of a Selective and Coke – Resistant MXene – Based Catalyst for the Dry Reforming of Methane", ACS Catalysis, Vol. 10, pp. 5124 – 5134, 2020. *https://dx.doi.org/10.1021/acscatal.0c00797?ref=pdf*

[6] X. Gao, J. Ashok and S. Kawi, "Smart Designs of Anti – Coking and Anti – Sintering Ni – Based Catalysts for Dry Reforming of Methane: A Recent Review", 2020.

[7] X. Gao, Z. Lin, T. Li, L. Huang, J. Zhang, S. Askari, N. Dewangan, A. Jangam and S. Kawi, "Recent Developments in Dielectric Barrier Discharge Plasma – Assisted Catalytic Dry Reforming of Methane over Ni – Based Catalysts", Vol. 11, No. 455, 2021. *https://doi.org/10.3390/catal11040455*